angular velocities Ω and $\Omega + \delta\Omega$ (assuming $\delta\Omega \ll \Omega$) is

$$\delta a_r = \frac{\Omega(\partial R^2/\partial r)}{(1-\Omega^2 R^2)}\,\delta\Omega\,, \tag{A4}$$

where $R \equiv -g_{\phi\phi}/g_{tt}$. We see that the acceleration is the same for all the observers (with $\Omega \neq \pm 1/R$) on a given orbit if and only if $\partial R/\partial r = 0$ on this orbit. Note, that on a free photon orbit we have $u^i u_i = 0$ and $a_i = 0$. Therefore $\Omega = \pm 1/R$ and $\partial R/\partial r = 0$ there. Thus, we have formally proved that observers (e.g., spacecraft) moving on a circular photon orbit with different angular velocities have exactly the same acceleration. It is *not* equal to the acceleration of the photons (which is zero) because of the assumption $\Omega \neq \pm 1/R$ one must make to derive formulas (3) and (4).

In the special case of the nonrotating black hole with the mass M:

$$g_{tt} = [1-(2GM/c^2 r)]c^2, \quad g_{\phi\phi} = r^2 \sin^2\theta \tag{A5}$$

and the condition $\partial R/\partial r = 0$ reduces to the formula for the radius of the photon orbit quoted in the paper:

$$r_c = 3GM/c^2\,.$$

The acceleration formula (3) gives

$$a_r = c^4/6GM\,,$$

which is independent of the angular velocity.

One could have the impression that these results are not covariant, that they are an artifact of the special coordinate system used. This is not the case. It is easy to express all the formulas presented here in terms of two Killing vector fields, η^i and ξ^i, which exist in the space-time with the metric (A1) because of time and axial symmetries. These two Killing vectors in the special coordinates connected with (A1) have the form:

$$\eta^i = \delta^i(t)\,, \quad \xi^i = \delta^i(\phi)\,,$$

with $\delta^i(k)$ being the Kronecker delta.

The formulas for angular momentum and angular velocity read:

$$1 = -\frac{(\xi^i u_i)}{(\eta^k u_k)}, \quad \Omega = -\frac{1(\eta^i \eta_i)}{(\xi^k \xi_k)}\,,$$

and the acceleration formulas take the form:

$$a_i \equiv u^k \nabla_k u_i = \frac{1}{2}\frac{\nabla_i(\eta^k\eta_k) + \Omega^2 \nabla_i(\xi^k \xi_k)}{(\eta^j\eta_j) + \Omega^2(\xi^j\xi_j)}\,,$$

$$\delta a_i = \frac{\Omega \nabla_i R^2}{(1-\Omega^2 R^2)}, \quad R^2 \equiv -(\xi^i\xi_i)/(\eta^k\eta_k)\,.$$

On the photon orbit one has $\nabla_i R = 0$ and the acceleration

$$a_i = \frac{1}{2}\frac{\nabla_i(\xi^k\xi_k)}{(\xi^j\xi_j)}$$

does not depend on the angular velocity. This proves our point.

[a] Permanent address: Département d'Astrophysique Fondamentale, Observatoire de Paris-Meudon, 92195 Meudon Principal Cedex and Institut d'Astrophysique de Paris, 98 bis Bd. Arago, 75014 Paris, France.

[1] A. Einstein, *Relativity, the Special and the General Theory* (Methuen, London, 1964).
[2] H. Cohn, Am. J. Phys. **45**, 239 (1977).
[3] D. S. Koltun, Am. J. Phys. **50**, 527 (1982).
[4] S. Weinberg, *Gravitation and Cosmology* (Wiley, New York, 1972).
[5] M. A. Abramowicz and J. P. Lasota, Acta Phys. Pol. B **5**, 327 (1974).

Chaotic dynamics of a bouncing ball

N. B. Tufillaro and A. M. Albano
Department of Physics, Bryn Mawr College, Bryn Mawr, Pennsylvania 19010

(Received 13 June 1985; accepted for publication 11 November 1985)

An undergraduate experiment is described that illustrates the period doubling route to chaos in a simple dissipative mechanical system, a bouncing ball subject to repeated impacts with a vibrating table.

I. INTRODUCTION

The period doubling route to chaos has now been observed in an impressive number of experimental systems. Electrical,[1-6] optical,[7] hydrodynamic,[8] chemical,[8] and biological systems can all exhibit period doubling instabilities. A few recent articles in this Journal deal with the chaotic dynamics of nonlinear systems.[11,12] but recent discoveries in nonlinear dynamics are still not well known at the undergraduate level.

We have developed an undergraduate experiment that illustrates many of the ideas and methods used in describing nonlinear dissipative dynamical systems. The experiment consists of two parts. In the first part the students explore the "quadratic map"[13] on a microcomputer. Many aspects of the quadratic map are common to a large class of systems showing chaotic behavior. By studying the quadratic map, the students are introduced to the basic notions of deterministic randomness (i.e., chaos), subharmonic bifurcations, strange attractors, and the like.

These ideas are immediately applied to a simple mechanical system in the second part of the lab. The students ex-

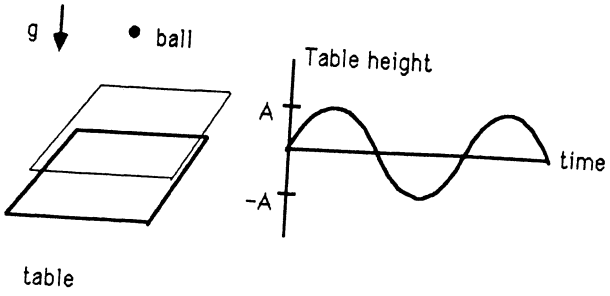

Fig. 1. Bouncing ball. A ball is free to bounce on a table which moves sinusoidally up and down.

perimentally study the dynamics of a ball that is free to bounce on a table which moves sinusoidally up and down (Fig. 1). The dynamics of a bouncing ball subject to repeated impacts with a sinusoidally vibrating table appears to have been studied first by Holmes[14] who showed the existence of periodic and chaotic motions (i.e., strange attractors) for suitable parameter values and initial conditions. The bouncing ball apparatus described here is simple, inexpensive, and exhibits period doubling. The students obtain an estimate of the Feigenbaum delta[15] from both the quadratic map and the bouncing ball experiment. The Feigenbaum delta measured from the latter consistently falls between four and five.

II. QUADRATIC MAP

Nonlinear dynamical systems are studied in two complementary ways by mathematicians and physicists. The *mathematical goal* of dynamical systems theory is to understand the asymptotic behavior of a dynamical process. The set of asymptotic solutions is called an "attractor." Attracting sets come in many varieties: fixed points, limit cycles, and strange attractors, to name a few. In physics, a dynamical process is oftened modeled by a differential or a difference equation, so the task before the mathematician is to find where all the orbits go after a long time. Physicists ask a more subtle (and ambiguous) question. One of the *physicist's goals* in nonlinear dynamics is to identify what such systems have in common, irrespective of differences in the underlying physics. A physicist seeks to discover those properties that are experimentally measureable and commonly realized in physical phenomena. This is the quest for universality. A familiar result is that a period doubling cascade can culminate in chaos. Moreover, this doubling cascade possesses certain universal, and experimentally realizable, scaling properties. These scaling laws were first noticed by studying the "quadratic map." For an eminently readable introduction to this, and related topics, see R. D. Hofstadter's "Metamagical Themas" in the November 1981 issue of *Scientific American* (Ref. 19).

The difference equation,

$$x_{n+1} = \lambda x_n (1 - x_n) \tag{1}$$

is called the "quadratic map." It is the simplest nonlinear one dimensional map imaginable. Unlike the analogous differential equation,

$$\frac{dx}{dt} = \lambda x(1 - x), \tag{2}$$

whose solution is simply

$$x(t) = x_0 e^{\lambda t} / [1 - x_0 (1 - e^{\lambda t})], \tag{3}$$

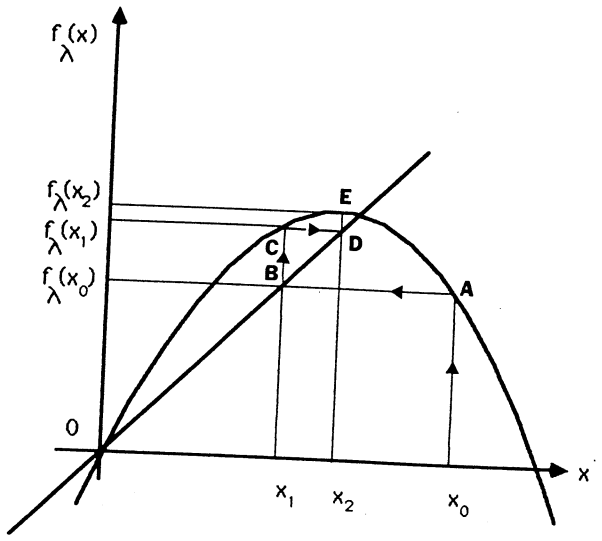

Fig. 2. The quadratic map. The first few iterates of x_0 are shown.

the solutions of the quadratic map can be astonishingly complex. In fact, some aspects of the asymptotic orbits are still not fully understood.

We can think of the quadratic map as a very idealized model of some dynamical process. It has, in fact, been used to model the temporal evolution of insect populations.[13,19] The parameter λ in this case may be a measure of the abundance and availability of food supplies which affects how large the next generation x_{n+1} will be given that the present population is x_n. In the bouncing ball experiment, λ might be the amplitude of the platform's oscillations, in hydrodyamic experiments, it might be the Reynolds number.

Much is learned about the quadratic map by examining the behavior of x_n starting from some arbitrary x_0. (In the following, we only examine the case where $\lambda > 1$.) A particularly simple graphical method for iterating Eq. (1) is illustrated in Fig. 2 (see Ref. 19) in which

$$f_\lambda(x) = \lambda x(1 - x) \tag{4}$$

is plotted against x. Starting from some x_0, the value of x_1 is obtained by drawing a line segment parallel to the $f_\lambda(x)$ axis from x_0 and extending it until it intersects the graph at A. The length of this line segment gives the value of x_1. The value of $x_2 = f_\lambda(x_1)$ is obtained by drawing a line segment parallel to the x axis from A until it intersects the diagonal, $f_\lambda(x) = x$, at B and then drawing the line BC. The height of C above the x axis gives x_2. All other future iterates, $x_3,\ldots,x_k,\ldots$ may be similarly obtained.

The first thing to notice is that $f_\lambda(0) = 0$. Thus if $x_0 = 0$, all future iterates remain at 0 and $x = 0$ is a trivial fixed point of the map. Next, if $x_0 < 0$ or $x_0 > 1$, then the future iterates of x_0 run away to negative infinity. Therefore, the interesting dynamics of the quadratic map are confined to the unit interval, [0,1]. Lastly, a nontrivial fixed point exists whenever $f_\lambda(x) = x$, i.e., whenever $f_\lambda(x)$ intersects the 45° line. Note that when $\lambda < 2$, no such intersections occur and all initial conditions on the unit interval converge toward $x = 0$ ($x = 0$ in this case is a *stable* fixed point) while for $\lambda > 2$, initial conditions near $x = 0$ diverge from it ($x = 0$ becomes an *unstable* fixed

```
10  XMAX = 250: YMAX = 179
20  INPUT "Enter lower lambda: "; llower
30  INPUT "Enter upper lambda: "; lupper
40  INPUT "Enter step size for lambda: "; lstep
50  HGR: HCOLOR = 3
60  FOR l = llower TO lupper STEP lstep
70      xplot = XMAX*(l - llower)/(lupper - llower)
80      x = 0.5
90      FOR i = 1 TO 200
100         x = l*x(1-x)
110     NEXT i
120     FOR i = 1 TO 200
130         x = l*x*(1-x)
140         yplot = YMAX*(1-x)
150         HPLOT(xplot, yplot)
160     NEXT i
170 NEXT l
180 END
```

Fig. 3. Bifurcation diagram program. The user inputs a minimum and maximum as well as a step size for lambda.

point) and all initial conditions seem to be attracted to other points.

After similar introductory remarks, the students are encouraged to explore the dynamics of the quadratic map on their own using a microcomputer. For instance, for various values of x_0 between zero and one, and λ between one and four, the students can watch the future iterates of Eq. (1) bounce around on the unit interval. They soon discover that if λ is between one and three then there exists only one attracting (stable) fixed point inside the unit interval and one repelling (unstable) fixed point at zero. That is, no matter what x_0 they pick, future iterates always go to where $f_\lambda(x) = x$. However, a more exciting result is obtained if $\lambda = 3.9$, say.

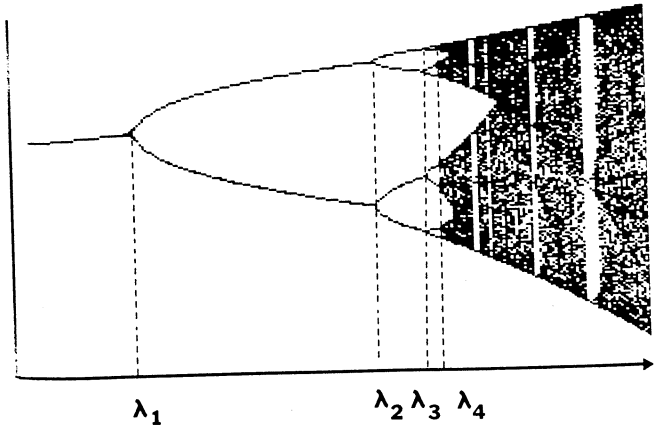

Fig. 4. Bifurcation diagram for quadratic map. The first pitch fork begins at λ_1. The second pitch fork (period $4T$) starts at λ_2.

Now that their curiosity is aroused, the students are guided to investigate systematically the dynamics of the quadratic map by constructing a "bifurcation diagram." This is a plot of x_n (for large values of n) versus λ. The program listed in Fig. 3 will run on any Apple II computer. (If hardcopy graphical output is desired, some graphical screen dump capability is required.) The graphical output is shown in Fig.4. The horizontal axis shows values of λ between 2.8 and 4. The vertical axis shows the attracting set on the unit interval for a given λ. The diagram was constructed by discarding the first two hundred iterates of x_0 (the transient solution) and then plotting the subsequent two hundred points. The bifurcation diagram displays how the attractor changes as λ increases.

Figure 4 illustrates the "period-doubling route to chaos" via a series of "pitchfork" bifurcations. For each value of $\lambda < \lambda_1$, the high-n limit set of the solution consist of a single point, called a period one solution: there is only one attracting fixed point. When $\lambda_1 < \lambda < \lambda_2$, a "period two orbit" exists, the solution hops back and forth between the upper and lower branches of the pitchfork. For $\lambda_2 < \lambda < \lambda_3$, a "period four" solution exists. This period doubling continues indefinitely, but the interval of a given periodic motion, $\lambda_n < \lambda < \lambda_{n+1}$, rapidly becomes more compact. λ_n soon converges to a value λ_c that marks the onset of chaotic behavior, at which point the iterates appear to randomly hop around on a subset of the unit interval. As λ is further increased, windows of periodic motion can reappear. In this regime, chaotic and periodic motion exist side by side.

Feigenbaum[15,20] discovered that the dimensionless number defined by

$$\delta_F = \lim_{n\to\infty} [(\lambda_{n+1} - \lambda_n)/(\lambda_{n+2} - \lambda_{n+1})] = 4.6692... \tag{5}$$

is independent of the details of the quadratic map. Furthermore, the convergence rate of Eq. (5) is quite rapid (quadratic, in fact). Hence, δ_F is well approximated by the first few values of λ_n. The students can obtain δ_F close to that given by Eq. (5) by using only the first few values of λ_n (e.g., $\lambda_1, \lambda_2, \lambda_3$) found in the quadratic map.

A remarkable feature of Feigenbaum's delta is its *universality*. It seems to characterize every dynamical problem that displays the period-doubling route to chaotic behavior. This is illustrated by the bouncing ball experiment which yields a value of δ_F that agrees with Eq. (5) to within roughly 10%.

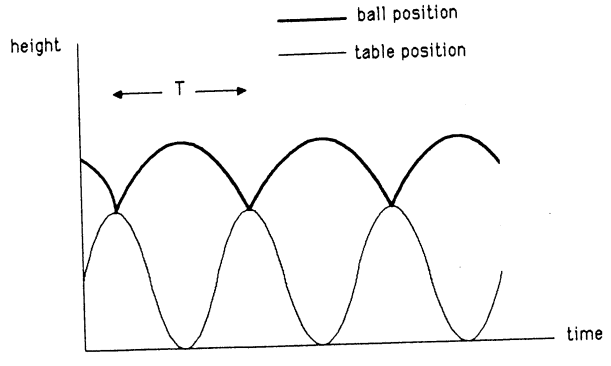

Fig. 5. Ball and table position. Periodic motion of period T is depicted.

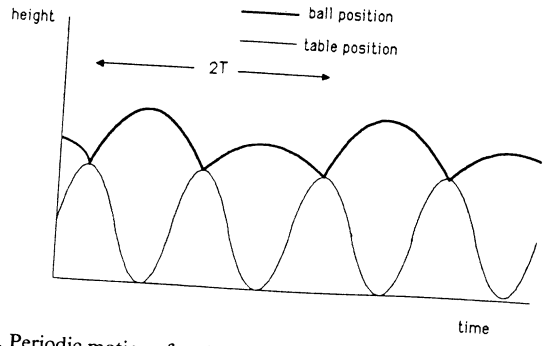

Fig. 6. Periodic motion of period $2T$.

III. QUALITATIVE DESCRIPTION OF A BOUNCING BALL

Imagine dropping a ball on top of a table that is oscillating in the vertical direction with a frequency ω and amplitude A (Fig. 1). In the bouncing ball experiment we want to study how varying the table amplitude A affects the ball's dynamics. The system is dissipative since the collisions are inelastic. We therefore expect the table and the ball to move in unison when A is small enough; no bouncing occurs. However, for a fixed ω and a large enough A, the ball will begin to bounce. As we shall see, the ball initially bounces periodically until we reach a critical value of the amplitude A_c at which point the ball bounces in a chaotic manner. New periodic and chaotic motions can appear if the amplitude increases further.

One way to visualize the ball's motion is to graph both the ball's height and the table's motion on the same plot. Figure 5 shows the simplest periodic motion we can imagine. The ball executes periodic motion with a period T equal to that of the forcing period. In Fig. 6, a $2T$ periodic orbit is illustrated; the ball bounces high, then low, then high again.

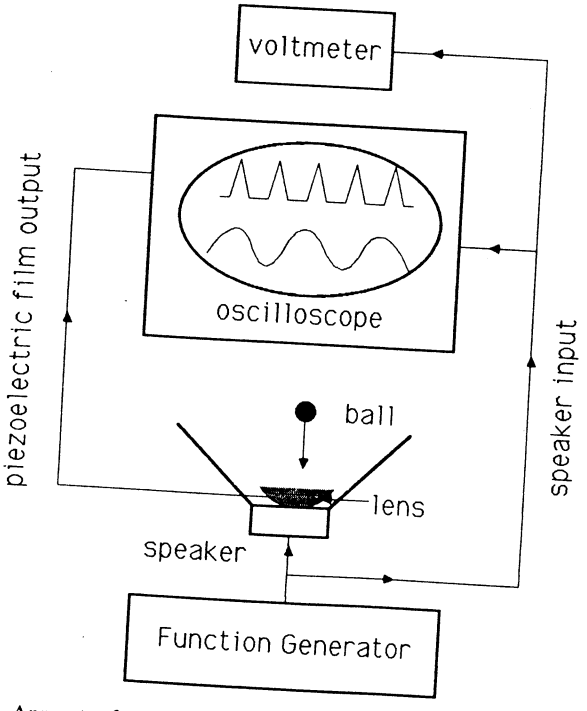

Fig. 7. Apparatus for bouncing ball experiment.

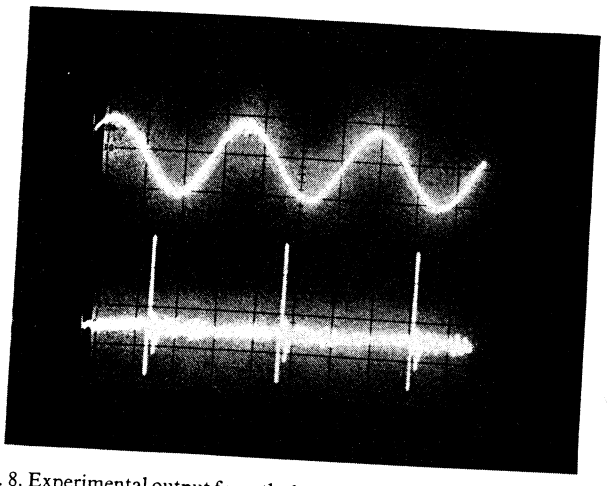

Fig. 8. Experimental output from the bouncing ball machine. A "T" periodic orbit is shown. The upper trace is the driving voltage to the speaker. The lower display shows the direct output from the piezoelectric film due impacts with the bouncing ball.

Studying the quadratic map showed us that the chaotic solutions were preceded by a sequence of period doubled solutions. Reasoning by analogy, we might guess that as we increase the table amplitude A—which is analogous to the parameter λ in the quadratic map—we will see a sequence of periodic orbits of periods T, $2T$, $4T$, $8T$, $16T$,... after which the ball moves chaotically. Notice that if the analogy is correct we will not see orbits of periods $3T$, $5T$, $6T$, $7T$,... in this sequence. Moreover, we can quantitatively test the analogy by calculating the Feigenbaum delta for the experimental system.

IV. BOUNCING BALL APPARATUS

A schematic diagram of a "bouncing ball machine" is shown in Fig. 7. A speaker driven by a function generator serves as the vibrating table. A small steel ball bounces against a concave lens glued to the speaker. The curvature of the lens helps to keep the ball's motion vertical. Fastened to the top of the lens is a thin ($28\,\mu$m) piezoelectric film.[16] Every time the ball hits the lens, the film generates a vol-

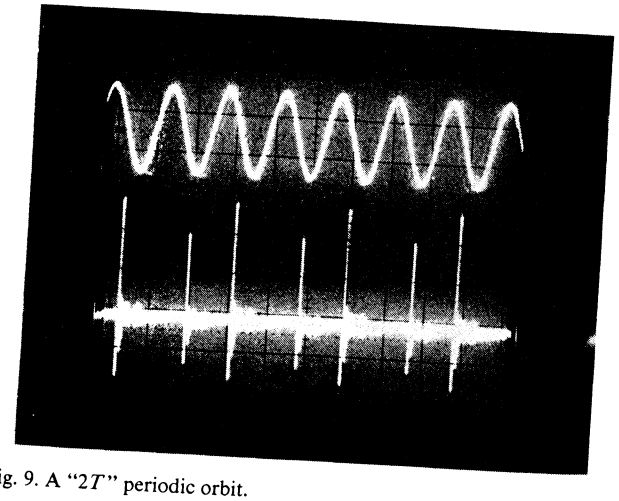

Fig. 9. A "$2T$" periodic orbit.

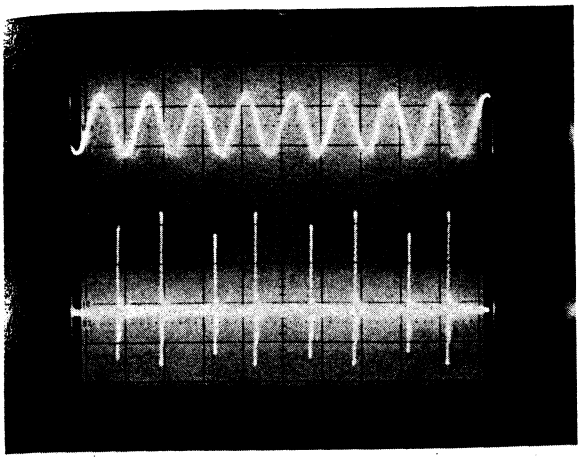

Fig. 10. A "$4T$" periodic orbit. The lower trace repeats itself at four times the forcing period.

tage, which is readily detected by an oscilloscope. The other channel of the oscilloscope shows the voltage driving the speaker. At impact, a sharp click is heard. The acoustical patterns of different periodic and chaotic motions are easily distinguished by the listener. The function generator is also connected to a voltmeter so that the driving voltage at a bifurcation value can be recorded.

V. BOUNCING BALL EXPERIMENT

With a frequency around 60 Hz, the students are asked to slowly increase and decrease the driving voltage while they practice listening for different periodic and chaotic motions. Once they hear a periodic pattern, the oscilloscopes is adjusted to trigger properly off the periodic signal. For small voltages, it helps to tap the speaker to start the ball bouncing. The students should note that the system displays hysteresis. The bifurcation points can differ for increasing and decreasing sweeps through A.

Actual experimental data of periodic motions of periods T, $2T$, and $4T$ are shown in Figs. 8–10, respectively. The upper trace displays the driving voltage fed to the speaker. The lower trace shows the signal generated by the piezoelectric film due to collisions with the bouncing ball. Presumably, the pulse height is proportional to the force of impact.

Once the students are familiar with the apparatus they are asked to construct a "bifurcation diagram" for the bouncing ball system similar to that shown in Fig. 11 by placing the function generator near its maximum value and then decreasing the amplitude noting for what voltages (read from the voltmeter) chaotic and periodic motions appear and disappear. The Feigenbaum delta can now be calculated and compared to the quadratic map result. Typical values (Fig. 11) give

$$\delta_F \approx (A_2 - A_1)/(A_3 - A_2) = 4.3. \tag{6}$$

The lab concludes with a few questions. For example, the students are asked to estimate the maximum separation between the ball and the lens by elementary considerations of projectile motion. Also they are asked to explain why long ($8T$, $16T$,..) periodic orbits are not seen in the experimental setup, i.e., why there is a trunction of the cascade.

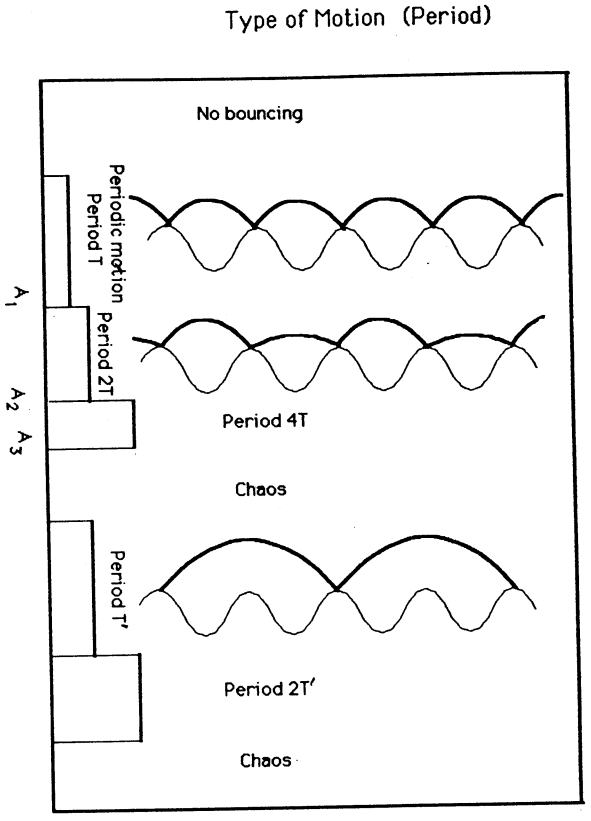

Fig. 11. Bifurcation diagram for bouncing ball experiment. Typical values are $A_1 = 0.149$ V, $A_2 = 0.226$ V, $A_3 = 0.244$ V.

VI. FUTURE WORK

A detailed analytic and numerical study of the bouncing ball system is in progress. Such a realistic model is not presented here in order to emphasize how much can be learned about the system by studying its analogies with the quadratic map. The more realistic model gives rise not to an interval map, but rather to a certain two-dimensional annular map.

In addition, we are currently engaged in a number of experimental studies. For instance, we are collecting data to calculate the fractal dimensionality[17] and distribution function of motion in the chaotic regime. The experimental result will be compared to those obtained from computer simulations. The bouncing ball system also provides a convenient system for testing new nonlinear phenomena such as noisy precursors of bifurcations discussed by Weisenfeld.[18]

ACKNOWLEDGMENTS

We thank the Physics 331 class of 1984-85 at Bryn Mawr College, especially Tina Mello and Lauree Shampine, for the testing of the original version of this experiment.

[1]P. S. Linsay, Phys. Rev. Lett. **47**, 1344 (1981).
[2]J. S. Testa, J. Perez, and C. Jeffries, Phys. Rev. Lett. **48**, 714 (1982).
[3]D. D'Humieres, M. R. Beasley, B. A. Huberman, and A. Libchaber, Phys. Rev. A **26**, 3438 (1982).
[4]S. Novak and R. G. Frehlich, Phys. Rev. A **26**, 3660 (1982).
[5]K. Aoki, K. Miyame, T. Kobayashi, and K. Yamamoto, Physica B

117&118, 570 (1983).
[6]S. W. Teitsworth, R. M. Westervelt, and E. E. Haller, Phys. Rev. Lett. **51**, 825 (1983).
[7]See N. B. Abraham, in *Fluctuation and Sensitivity in Nonequilibrium* (Springer, Berlin, 1984), p. 152, and reference therein.
[8]See H. L. Swinney, Physica **47**, 7D (1983), and references therein.
[9]M. Guerara, L. Glass, and A. Shrier, Science **214**, 350 (1981).
[10]L. Glass, M. R. Guerara, and A. Shrier, Physica **89**, 7D (1983).
[11]T. Mishina, T. Kohmota, and T. Hashi, Am. J. of Phys. **53**(4), 332 (1985).
[12]E. V. Mielczarek, J. Turner, D. Leiter, and L. Davis, Am. J. of Phys. **51**, 32 (1983).
[13]R. M. May, Nature **261**, 459 (1976). The quadratic map is also known as the logistic map.
[14]P. J. Holmes, J. Sound Vibration **84**(2), 173–189 (1982).
[15]M. J. Feigenbaum, Los Alamos Science **1**, 4 (1980).
[16]The KYNAR piezoelectic film is available from Pennwalt Corporation, 900 First Avenue, P.O. Box C, King of Prussia, Pennsylvania, 19046-0018. A 10 cm×20 cm sheet 28 μm thick with standard nickel–aluminum coating costs $35. The KYNAR Technical Manual is available from Pennwalt for $10 and lists suppliers for conducting adhesives.
[17]P. Grassberger and I. Procaccia, Phys. Rev. Lett. **50**, 346 (1983).
[18]K. Wisenfeld, J. Stat. Phys. **38**, 1071 (1985).
[19]D. R. Hofstadter, "Metamagical Themas," Scientific American (November, 1981) 22–43.
[20]M. Fiegenbaum, J. Stat. Phys. **21**, 669 (1979).

Derivation of the potential energy for the inverse square force—Without calculus

Jeffry V. Mallow
Department of Physics, Loyola University of Chicago, Chicago, Illinois 60626

(Received 4 October 1985; accepted for publication 19 December 1985)

A derivation is presented for the potential energy using the assumption of elliptical orbits for a mass under the influence of a $1/r^2$ force. This eliminates the need for a calculus-based derivation, and is therefore, appropriate for a wide range of nonmajors' introductory physics courses.

For the undergraduate who knows calculus, the derivation of the $1/r$ potential from the $1/r^2$ force is exceedingly simple: A single integration of $1/r^2$ between distances r_1 and r_2 yields $1/r_1 - 1/r_2$. For the students in non-calculus-based introductory physics courses, this simple derivation is inaccessible, and most texts either state the result, or implicitly or explicitly invoke calculus as part of a "derivation."[1]

In this paper, I derive the expression for ΔPE from examination of the properties of the elliptical orbit of a particle (charge or mass) subject to a $1/r^2$ attractive force. The only prerequisites are high school algebra and geometry, and the concepts of angular momentum and energy.

Consider a mass m orbiting a fixed mass M. The gravitational force $F = GMm/r^2$ produces an elliptical orbit, with M at one focus, as shown in Fig. 1. The semimajor axis is a, the semiminor axis is b, the eccentricity is e and the distances from M to the turning points are r_1 and r_2 ("perigee" and "apogee," respectively). Since gravity is a conservative central force, any conclusions we draw about the energies of m at r_1 and r_2 is true about any positions, not just the turning points, and for any motion of m, not just elliptical. Note from the geometry that

$$r_1 = a(1-e)\,,$$

$$r_2 = a(1+e)\,,$$

and

$$b = a(1-e^2)^{1/2}\,. \tag{1a}$$

(The distance from the focus to the intersection of the ellipse with the y axis is also equal to a, because the constant "length of string" between foci is $2a$). Thus

$$b = (r_1 r_2)^{1/2}$$

and

$$a = (r_1 + r_2)/2\,. \tag{1b}$$

We choose to investigate the motion of m at the turning points, because at these positions, velocities v_1, v_2 are perpendicular to distances r_1, r_2, and the motion is therefore centripetal.

Writing $\Delta PE = -\Delta KE$,

$$\Delta PE = PE(r_2) - PE(r_1) = m(v_1^2 - v_2^2)/2. \tag{2}$$

Now at r_1 and r_2, m may be considered to be in a circular orbit of radius $\bar{r}$, subject to the gravitational force (see Fig. 1):

$$v_1^2/\bar{r} = GM/r_1^2$$

and

$$v_2^2/\bar{r} = GM/r_2^2\,. \tag{3}$$

(Note that $\bar{r}$ is the same for both positions, since $v_1 r_1 = v_2 r_2$ from angular momentum conservation.)

Thus, from (2) and (3)

$$\Delta PE = (GMm/2)\bar{r}(1/r_1^2 - 1/r_2^2)\,. \tag{4}$$

It now remains to determine $\bar{r}$. This can be done by comparing the expression for the circle of radius $\bar{r}$ centered at $(a-\bar{r},0)$ to that for the ellipse, as $(x,y)\to(a,0)$:

$$[x-(a-\bar{r})]^2 + y^2 = \bar{r}^2 \tag{5}$$